DC-Bus Signaling control laws for the operation of DC-microgrids with renewable power sources

Iván Patrao, Enric Torán, Raúl González-Medina, Marian Liberos, Emilio Figueres. *Member, IEEE*. Gabriel Garcerá, *Member, IEEE.*

***Abstract*— DC-Bus Signaling (DBS) is a proven method to coordinate different microgrid agents, using the DC voltage of the microgrid as a communication signal. The droop control applied in a DC microgrid achieves accurate power-sharing among converters while leading to a certain voltage regulation error in the microgrid bus. The behaviour of the different agents in a microgrid is managed by using the voltage at each node of the microgrid as the DBS signal. The technique proposed in this paper uses an improved DBS technique to coordinate interlinking converters, photovoltaic generators, Energy Storage Systems and loads in a microgrid.**

The operation of the renewable power sources of a microgrid at the full generated power is desired due to economic and environmental reasons. The DBS technique proposed in this paper is adapted to integrate renewable power sources in the microgrid. The DBS-controlled Energy Storage Systems (ESS) will store the surplus energy if the generated power exceeds consumption. In the case of fully charged ESS, the renewable generators will limit their output power to those demanded by the loads. The proposed control laws have been tested in an experimental microgrid.

***Index Terms*— DBS, dc-bus, microgrids, power, sharing, droop, load, management**

I. INTRODUCTION

COOPERATION of small-scale generators (renewable or not) and mid/big-scale generators forming a microgrid is the new paradigm in energy management [1,2, 3]. The microgrid performance can be boosted by dynamic load management [4,5] in coordination with energy storage systems (ESS) [6]. Intelligent control of generators, loads and storage systems leads to excellent grid quality, reliability and lower exploitation costs and CO_2 emissions.

A microgrid has different agents distributed among a physical area (generators, ESS and loads). However, these agents must work together to operate the microgrid within the desired parameters of robustness and stability [7, 8]. The coordination system often uses communication links between the agents in a microgrid, but they are a critical issue due to costs, delays, and reliability [8]. Hence, communication links should be avoided if it is possible. Otherwise, low-speed fault-tolerant communication links should be used [9, 10].

Microgrid generators frequently use the droop control technique [11]. However, the operation of distributed generators under droop laws leads to a degradation in voltage accuracy. Moreover, power-sharing among the different converters in the microgrid is a critical issue. Consequently, many papers dealing with communications have been published to reduce voltage error and improve load-sharing accuracy [12].

Since the communication links increase the cost and reduce the reliability of the overall system, the operation based on terminal values (i.e., DC voltage of the microgrid) of the agents of the microgrid is desired. In the DC-Bus Signalling (DBS) method, the agents adjust their operation mode based on their own terminals' voltage value. The DBS method often coordinates the different types of generators and loads in DC microgrids [13-15].

In the literature, it's possible to find various proposals for secondary control [16] using the bus voltage to coordinate the operating mode and power-sharing in DC microgrids. A Voltage-Level Signaling (VLS) technique has been proposed in [14,17]. In this method, the voltage variation of the DC-bus is divided into windows, each assigned to specific operating modes. It's a cheap and easy-to-implement control method, but the achieved power-sharing is poor, and a vast number of paralleled converters may lead to excessive voltage windows. DBS is created by combining VLS and Droop methods [18]. Hence, in DBS every change is progressive among operating states. Later, [19] presented an evolution of DBS called Mode-selective DBS. The approach of this method is to decide which converter operates as a voltage source according to the DC-bus voltage, while the rest serve as current sources. Modifications with advanced features have been proposed recently [20], like Communicative DBS, where voltage variations serve as a low-speed digital communication link.

Regarding VLS [14, 17], the technique proposed in this paper uses a minimal number of voltage windows while providing a smooth behaviour. To achieve this performance several DBS control laws for the agents in a DC microgrid are proposed. Each control law fits the specific characteristics of the typical agents in a microgrid (interlinking converters, energy storage systems and renewable energy sources). Compared with the Mode-selective DBS [19], in the proposed technique all the generators behave as voltage sources, thus avoiding the master-slave or grid-forming/grid-following problems. Thus, a fully decentralized power-sharing algorithm performs the voltage regulation of the microgrid. Compared

This research was funded by the Spanish "Ministerio de Asuntos Económicos y Transformación Digital" and the European Regional Development Fund (ERDF) under Grants RTI2018-100732-B-C21 and PID2021-122835OB-C22.

The authors are with: Grupo de Sistemas Electrónicos Industriales del Departamento de Ingeniería Electrónica, Universitat Politècnica de València. Camino de Vera s/n, 46022 Valencia (Spain). Corresponding autor: Iván Patrao (ivpather@upv.es).

with the Communicative DBS [20], no master module or communication links between agents are required. Thus, a Plug-and-Play DC microgrid is possible since any converter does not need to be informed about the characteristics of the rest of converters.

Unlike frequency in AC systems, the node voltage is not a global measurement but a local parameter, providing information about the state of charge of each node. For instance, a low voltage stands for a highly loaded node, while a high voltage stands for a poorly loaded one.

The control technique proposed in this paper proves to be a feasible method for the coordination and power management of renewable sources in a microgrid. The DBS control technique can coordinate the renewable generators and ESS devices to store the excess in production or limit the energy production in the case of full charged ESS.

.II. DC-BUS SIGNALLING (DBS)

The DBS method uses the DC bus voltage as a reliable parameter of the microgrid operating conditions. The voltage value measured at the output terminals of each converter determines the operating mode [14]. In the classical DBS method, the master converter usually establishes the microgrid DC voltage, and the rest of the converters in the microgrid operate according to this voltage level. For instance, the diesel generators in a microgrid will only work below a certain voltage level, remaining idle for voltages above that level. Some variations of this method have been presented [15].

Most DC buses are specified with a broad tolerance ratio since the agents connected to the microgrid have a dc/dc power converter with a wide input voltage range. In the DBS technique, such voltage error determines the operating mode of the agents in the microgrid.

The IEEE Standard 1547 limits the microgrid DC voltage variation between 0,95 and 1,05 p.u. For instance, the voltage of a 450 V_{DC} microgrid can swing between 427,5 V_{DC} and 472,5 V_{DC} under normal circumstances. Various published works try to use communication links to reduce this voltage error to very low values [21], but this is far beyond the objective of the standard.

The DBS technique takes advantage of this voltage deviation and uses it as a flag of the microgrid status. Moreover, due to the resistive behaviour of the power transmission lines, the voltage of each node serves as an indicator of the node's state of load. Voltages near the highest limit (about 470 V_{DC}) suggest that this microgrid node drains only a small part of the available power. Voltages near the lower limit (about 430 V_{DC}) suggest that the load is close to the maximum node capacity. Thus, microgrid agents can decide how to act according to the voltage measured at their output (terminal values).

The 450 V_{DC} nominal value used in this work is in the range of the typical microgrid examples, but the results are independent of the nominal value used in the tests. Hence, both low-voltage and high-voltage DC microgrids can implement this technique.

The linear behaviour of the DBS technique can be modelled as (1), being P_{MAX} the nominal power of the converter, ΔP and ΔV the maximum variations of power and voltage, V_{NODE} the microgrid measured voltage, and V_{min} the minimum affordable voltage at this node. Since the DBS technique relies on the error deviation to adjust the output power reference, the measurement error in the voltage signal can affect the performance of the power-sharing technique. From (1), it can be deduced the power perturbation equation (2) and the effect of the voltage deviations (3), where ΔV represents the node voltage variation, and V_{ERROR} is the measurement error in the voltage signal. Since the same coefficient ($\Delta P/\Delta V$) affects the error and voltage variations, its influence on the output power reference is similar. Hence, the DBS technique requires better accuracy of voltage sensing circuits than the nominal voltage variation.

$$P_{REF} = P_{MAX} - \frac{\Delta P}{\Delta V} \cdot (V_{NODE} - V_{min}) \quad (1)$$

$$\Delta P_{REF} = \frac{-\Delta P}{\Delta V} \cdot (\Delta V) \quad (2)$$

$$\Delta P_{REF} = \frac{-\Delta P}{\Delta V} \cdot (\Delta V) + \frac{-\Delta P}{\Delta V} \cdot (V_{ERROR}) \quad (3)$$

Considering a microgrid formed by two converters of the same nominal power (P_N), delivering P_1 and P_2 output power, (4) and (5) are obtained. The influence of the voltage sensing error is represented in (5) as a voltage offset. Thus, the microgrid node voltage can be calculated as (6), where P_T represents the load power. The generalization of this equation for any number (N) of identical paralleled DBS-controlled converters leads to (7). Hence, it is demonstrated that the voltage error in the sensing circuits could significantly affect the power delivered by a converter. However, its effect on the voltage regulation of the entire microgrid is smaller as the number of converters increases.

$$P_1 = P_N - \frac{\Delta P}{\Delta V} \cdot (V_{NODE} - V_{min}) \quad (4)$$

$$P_2 = P_N - \frac{\Delta P}{\Delta V} \cdot (V_{NODE} + V_{error} - V_{min}) \quad (5)$$

$$V_{NODE} = \left(P_N - \frac{P_T}{2}\right) \cdot \frac{\Delta V}{\Delta P} + \frac{V_{error}}{2} + V_{min} \quad (6)$$

$$V_{NODE} = \left(P_N - \frac{P_T}{N}\right) \cdot \frac{\Delta V}{\Delta P} + \frac{V_{error}}{N} + V_{min} \quad (7)$$

III. PROPOSED CONTROL TECHNIQUE

The voltage swing of the microgrid DC voltage (from 430 V_{DC} to 470 V_{DC}) is divided into different working areas, as shown in Table I (microgrid nominal voltage: 450 V_{DC}). Minor voltage variations around its nominal value (+/-10 V_{DC}) are considered mid-power operation mode: the generators have enough power to feed the loads. If the voltage falls below the -10 V_{DC} deviation, the microgrid generators still power the loads, but their output almost reaches its maximum capacity. If the loads demand more power, the microgrid generators could not be able to provide it. On the contrary, if the voltage exceeds the +10 V_{DC} deviation, the

microgrid has light-load conditions, and the generators have significant available power.

TABLE I
MICROGRID VOLTAGE WORKING AREAS

Microgrid voltage	Description
V_N-20 V < $V_{MICROGRID}$ < V_N-10 V (430 V_{DC} < $V_{MICROGRID}$ < 440 V_{DC})	The power demanded by loads is almost equal to those available in generators.
V_N-10 V < $V_{MICROGRID}$ < V_N+10 V (440 V_{DC} < $V_{MICROGRID}$ < 460 V_{DC})	Mid power operation
V_N+10 V < $V_{MICROGRID}$ < V_N+20 V (460 V_{DC} < $V_{MICROGRID}$ < 470 V_{DC})	A great amount of available power is in the generators.

In this work, the control algorithm of each converter calculates the power to be delivered using the node voltage measurement. This technique leads to a wireless power-sharing behaviour. Moreover, the microgrid DC voltage is used to adjust the operating mode of some converters; for instance, the ESS charges the battery for high voltage values and discharges the battery to provide power support for low voltage values. We present control laws for interlinking converters, photovoltaic power sources and energy storage systems (ESS). Moreover, the loads use this node voltage value to decide whether they must remain connected or be disconnected to prevent the collapse of the microgrid. The definition of four different priority levels will determine the management of such loads. The trip voltage values proposed in this paper are shown in Figure 1, which are established so that the performance of each agent is optimized to reinforce the microgrid's stability. The behaviour of any type of agent is based on those presented in [22], but in the following sections it is revised and complemented.

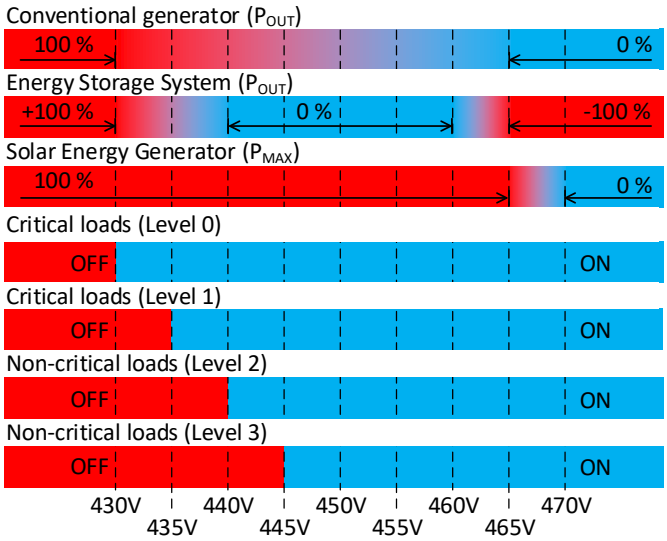

Fig. 1. DBS trip voltage values (nominal voltage: 450 V_{DC}).

When some generators lose their power capacity, the DBS load-managing technique disconnects the loads based on their priority, adapting the consumption to the available power. So, the loss of any generator's capacity is not a critical issue since the worst scenario leads to the disconnection of loads based on a prioritized level of importance.

A. Interlinking converters

The interlinking converters, seen in the dc-microgrid as DC sources, will operate as power sources dependent on the microgrid node voltage (terminal voltage value). The proposed operation range is 430-465 V_{DC} with a linear voltage-to-power behaviour. For voltages above 465 $V_{DC,}$ the power delivered is zero (0%), while for microgrid voltages below 430 $V_{DC,}$ the output power is maximum (100%). Figure 2 shows the proposed control law for interlinking converters.

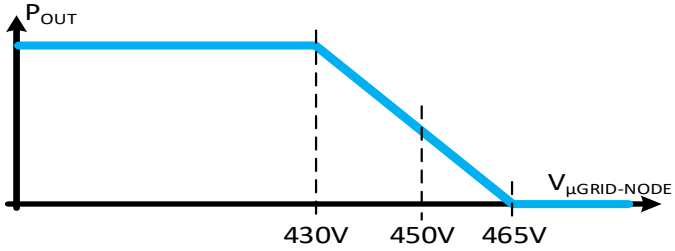

Fig. 2. DBS control law for interlinking converters.

Thus, a DBS linear control law sets the power reference used to generate the output current reference value for the operation of the interlinking converter.

Since there is no voltage loop, the microgrid DC voltage is not directly controlled, but it will be established at the point where the power injected into the microgrid equals the loads' consumption. Adding more converters in the microgrid does not change the control law. Moreover, an extra power injection (new converter) increases the microgrid DC voltage and, thus, reduces the power delivered by the rest of the converters, leading to a new operating point.

The power converters operating under DBS control must behave as current sources using an internal control loop fed by a current reference. The current compensator processes this reference and provides input for the PWM modulator, thus generating the gate-switching signals. Figure 3 depicts the control structure proposed for a power converter working under DBS law, in which the DBS control processes the sensed microgrid node voltage to generate the power reference. The division of the power reference by the measured voltage generates the current reference value. This reference is then limited to the maximum/minimum values the converter accepts and fed to the inner current control loop. The current control allows the converter to operate safely at any output conditions, even under short-circuit.

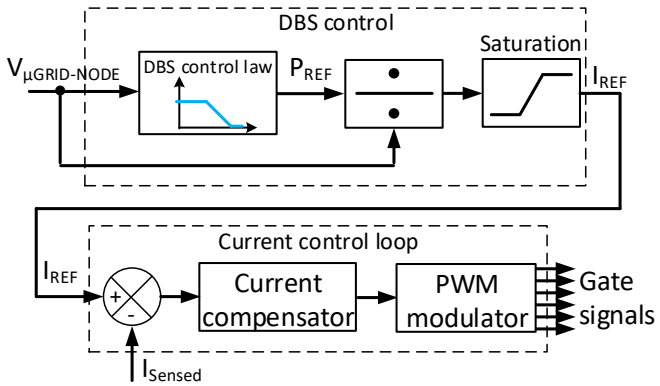

Fig 3: Power control loop based on DBS

Due to the resistive characteristic of the wires in low-voltage DC microgrids [23], the nodes with a higher load will exhibit a lower voltage. Since DBS establishes a direct relationship between voltage and power, the power-sharing among generators won't be accurate. However, those placed near the higher loads will deliver a more significant amount of power, thus reducing the wiring power losses.

Suppose the full load of a microgrid is concentrated at a point far away from the most powerful converters. In that case, the DBS technique will lead to a poor voltage in the DC bus, exceeding the acceptable voltage deviation limits. Low-bandwidth non-critical communication links can correct this undesirable behaviour. However, this is not a realistic scenario since the consumption in a microgrid tends to be distributed, and in most real situations, there is no need for a communication link.

B. Plug-in Electrical vehicle (PEV) and other energy storage systems (ESS)

Microgrids can lack peak-power capacity under certain circumstances due to their limited number of generators, i.e., during motor start-up or heavy transients in general. The massive integration of Plug-in electrical vehicle (PEV) in microgrids is a major challenge due to its high-power demand. Thus, the correct scheduling of its charge/discharge performance is critical for the microgrid's robustness [24].

The microgrid planning classifies the high storage capacity of the PEV as an Energy Storage System (ESS), which can provide support during heavy power transients. The Vehicle-to-Grid (V2G) [25] concept states that the charge of the PEV battery must be scheduled according to the microgrid capacity at any moment. Thus, a fully charged battery discharges to support the microgrid, performing as an energy buffer. The integration of the PEV in the grid is studied under the V2G and Vehicle-to-Building (V2B) terms [26,27].

The key point is to charge the battery of the PEV when the microgrid is under low load (i.e., high microgrid voltage, >460 V_{DC}); thus, the PEV charging power demand does not affect the microgrid's maximum peak-power capacity. Then, the PEV must be ready to return a portion of its charge to the microgrid if the load approaches the total power capacity on the node of the microgrid (i.e., low microgrid voltage, <440 V_{DC}). In the mid-power operation, the PEV battery does not charge/discharge, reserving the available power for the regular microgrid operation.

ESS will work under the control law shown in Figure 4. A node voltage around the nominal value sets a zero-power reference for ESS. A high voltage value sets a charging current, higher as the microgrid's available power increases. For instance, when a vast amount of photovoltaic energy is available in the microgrid. A low voltage value sets a discharging current, higher as the microgrid's available power decreases. The State-of-Charge (SoC) of ESS establishes limits for the maximum current to be supplied/drawn from the battery. Hence, the maximum charge ($P_{ch\text{-}MAX}$) or discharge ($P_{DIS\text{-}MAX}$) power of the PEV battery will be adjusted, even dynamically, according to the ESS SoC.

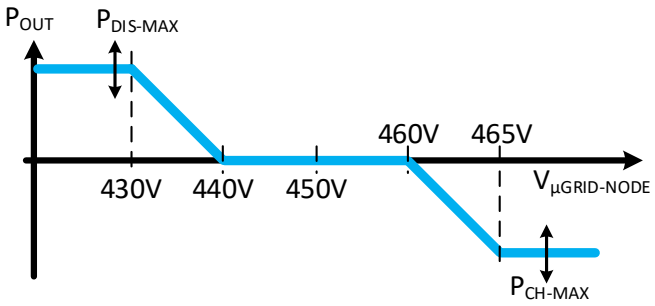

Fig 4: DBS control law for PEV and ESS

In the case of a full battery, the $P_{CH\text{-}MAX}$ value is set to zero; hence, the converter won't charge the battery. Similarly, below a specific value of SoC, the P_{DIS_MAX} value is also set to zero, and then the converter won't deliver any energy to support the microgrid.

C. Photovoltaic energy sources

Integrating renewable energy sources in microgrids is complicated due to the unpredictable generation and the limited load capacity. Correct microgrid management must ensure that the renewable sources operate at their full available power, feeding the loads and storing the excess energy produced in the ESS systems. When ESS are full, and the load demands less power than those generated by renewable sources, the microgrid must be able to limit the output power of such converters, ensuring a good power quality to the loads. In this research, the DC microgrid integrates PV energy sources.

Small photovoltaic (PV) power plants are used as low-power distributed energy power sources in most microgrids. Moreover, microgrid management must prioritize the solar energy of a microgrid since its energy source is free, thus lowering the exploitation cost and improving the environmental impact of the microgrid. However, the mismatch between solar energy and power consumption complicates its utilization in microgrids. Thus, coordinating the PV generators with the ESS leads to higher solar-energy production.

If the PV generation in a microgrid represents only a tiny percentage of the overall power, the PV generators usually operate at their MPP. As the microgrid demands more power than those produced in the PV generators, there is no need to limit its output. However, when the PV generation reaches high percentages of the installed power, the PV power is expected to exceed the power required by the loads. In such a scenario, the ESS systems must store the excess energy; if it is not possible, the power production must be limited. The proposed DBS law manage loads, ESS and PV generators.

A photovoltaic power converter in a microgrid should behave as follows: running the Maximum Power Point Tracking (MPPT) algorithm when the microgrid can absorb the generated power and limiting the power obtained from the solar modules when the microgrid is not able to absorb it.

In DBS, the microgrid's voltage provides information about the stage-of-load of the microgrid, so it is possible to define

some trip voltage values to coordinate and limit the behaviour of ESS and PV generators. The trip voltage at which the photovoltaic converters limit their output power is set up higher than those for the maximum charging power in the ESS. Hence, the PV converters will operate at the MPP while the ESS charge at their full power capacity if there is excess energy production. When there is no load nor ESS capacity to absorb the PV production, the output power of the PV generators is limited, as depicted in Figure 5. The slope between 465 V_{DC} and 470 V_{DC} allows equalisation of the loads connected to the microgrid and smoothing of transients.

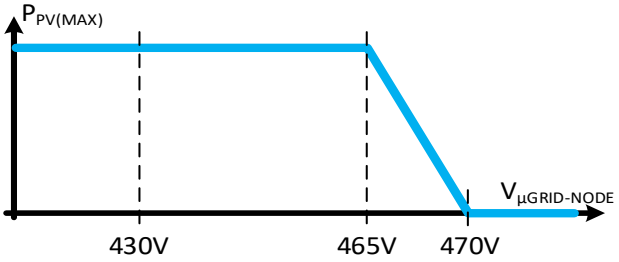

Fig 5: DBS control law for PV generators.

Figure 6 depicts the MPPT algorithm proposed for the PV generators running under DBS in the DC microgrid. It is based on the classical Perturb&Observe (P&O) method [28]: The voltage reference value is perturbed by a step (ΔV_{PV}), then the system evolves to a new PV voltage value and the new power is calculated. If the power obtained is increased, the sign of the step is kept; otherwise, it is changed. However, an extra condition has been added ($P_{PV(K)} > P_{PV(MAX)}$) to operate outside the Maximum Power Point (MPP) when the microgrid voltage is higher than 465 V_{DC}. The DBS control law establishes the $P_{PV(MAX)}$ value and limits the maximum power obtained from the PV generator according to the DBS law.

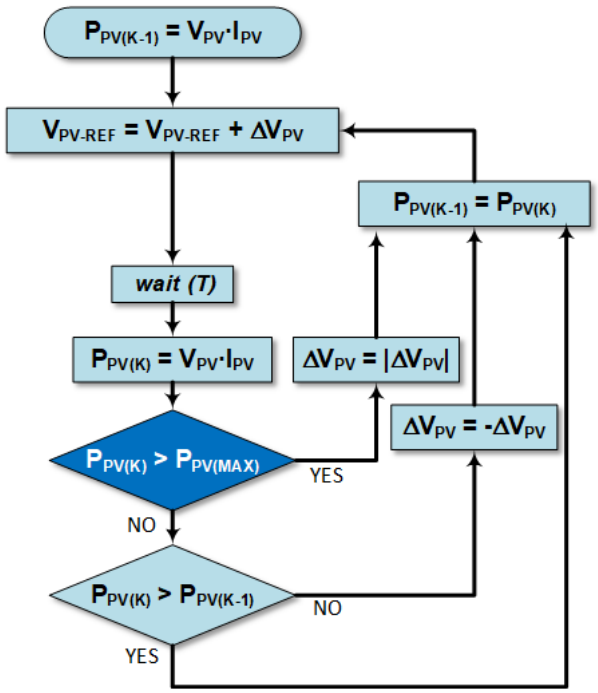

Fig 6: MPPT algorithm for DBS PV generators.

C. Loads

Along with generators and ESS management, load management improves the microgrid robustness against power peaks.

Loads can be classified into critical and non-critical ones. Critical loads must always be powered, while non-critical loads can be disconnected when sufficient power is unavailable in the microgrid's node. Using the DBS technique in each load controller, the status of the microgrid node is estimated, and the load can decide to connect/disconnect.

The microgrid must guarantee enough power to feed the critical loads, traditionally through diesel power generators, running only during critical scenarios. Examples of critical loads are lighting, computers or medical equipment.

The non-critical loads can be disconnected from the microgrid if the voltage is too low since the microgrid is near to collapse. When the microgrid power capacity increases (for instance, because of a critical-load disconnection), the non-critical loads can be connected again. Examples of non-critical loads are water heaters or air conditioners.

Various priorities for loads can be defined to provide accurate load priority scheduling. The authors propose two levels for critical loads (levels 0 and 1) and two levels for non-critical loads (levels 2 and 3). Table II shows the trip voltages for the different types of loads. A hysteresis of ±1V in a V_{DC} filtered measurement is proposed for stable load connection/disconnection operation.

TABLE II
Priority level for loads

Microgrid trip voltage	Description
Level 3: non-critical loads (V > 445 V_{DC})	Non-critical loads can be connected when a significant amount of power is available in the microgrid.
Level 2: non-critical loads (V > 440 V_{DC})	Non-critical loads generate only a minor inconvenience if disconnected for some time.
Level 1: critical loads (V > 435 V_{DC})	Critical loads that can be disconnected, if necessary, with a limited inconvenience
Level 0: critical loads (V > 430 V_{DC})	Critical loads that cannot be disconnected from the microgrid. Disconnected only if the microgrid is about to collapse.

IV. Experimental Results

A. Microgrid structure and equipment

The experimental DC-microgrid used to validate the DBS technique has two nodes with three power converters (overall power of 10 kW), which are connected as shown in Figure 7. Different loads are connected in the nodes. Both converters and loads work according to their terminal's voltage, using the voltage of the microgrid nodes as a microgrid status indicator. The dc-bus is set to 450 V_{DC} +/- 20 V.

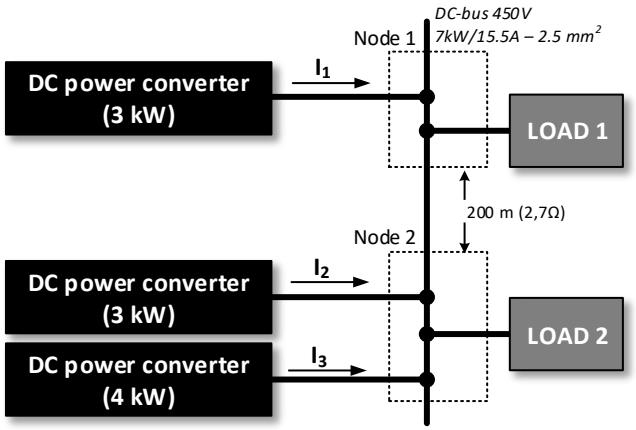

Fig 7: Physical structure of the tested microgrid

The wire impedance of the power transmission line between nodes #1 and #2 is emulated to provide realistic results. A long line (200 m) of 7 kW (15,5A/450 V_{DC}) nominal power is supposed. So, the required section in the wiring is 2,5 mm^2 (material: aluminium). Since the inductance of an electrical low-voltage transmission line is estimated as 318 µH/km [29], it is neglected in low-voltage microgrids due to its limited length. Generally, in such lines, the inductive part of the impedance is much lower than the resistive one. Hence, a 2,7 Ω resistor emulates the line impedance.

We have tested three types of converters: interlinking converters, ESS systems and photovoltaic generators. With minimal modifications, the hardware is similar for all of them, adapting the control scheme to the required function. The converters are configured to behave as interlinking converters, PV generators or ESS as needed for each test. The power stages are 3-phase full-bridge topologies designed for a maximum output power of 10 kW but limited to 3 kW/4 kW in the tests that have been carried out. The maximum DC voltage is 750 V.

Interlinking converters are built up by means of a grid-tied three-phase inverter, following Fig. 8. The DBS control law determines the power set point and calculates the current reference. Figure 8 depicts the hardware configuration and the control scheme of this type of agent.

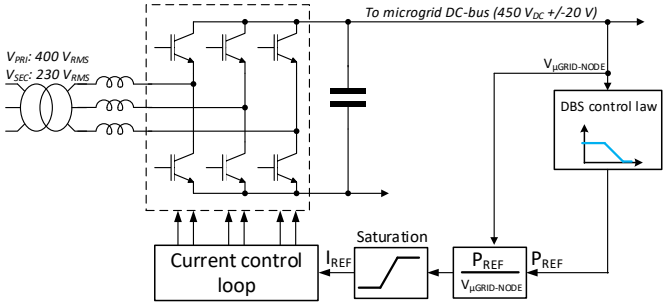

Fig 8: Interlinking converter: hardware and control scheme.

ESS units are built-up by using a single leg of the same power stage as for interlinking converters. The measured microgrid DC voltage and the SoC of the battery determines the power set-point, through the DBS control law. Then, the current reference is calculated. The inner current control loop ensures good tracking of such reference. Figure 9 depicts the hardware configuration and the control scheme of this type of agent.

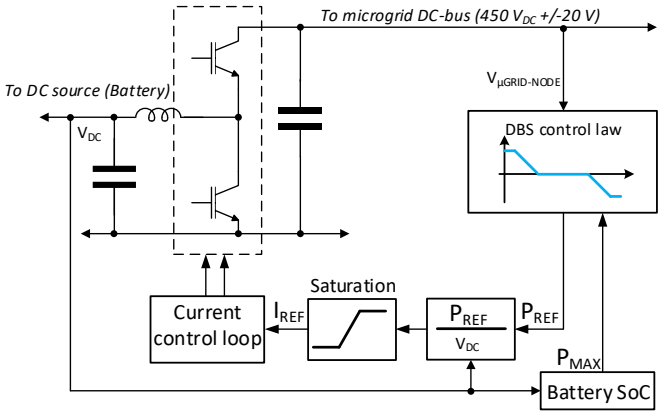

Fig 9: ESS: hardware and control scheme.

The solar energy generator is built-up by means of the same hardware used for ESS, but the control loops are adapted to the required functionality (see Figure 10). The measured microgrid DC voltage determines the maximum allowed power. Next, the MPPT algorithm presented in the previous section establishes the voltage reference, and the voltage control loop calculates the current reference. The inner current control loop ensures good tracking of such reference. The PV source is emulated by means of a TerraSAS ETS 1000/15 PV simulator, capable of emulating V-I curves and irradiance/temperature dynamic variations.

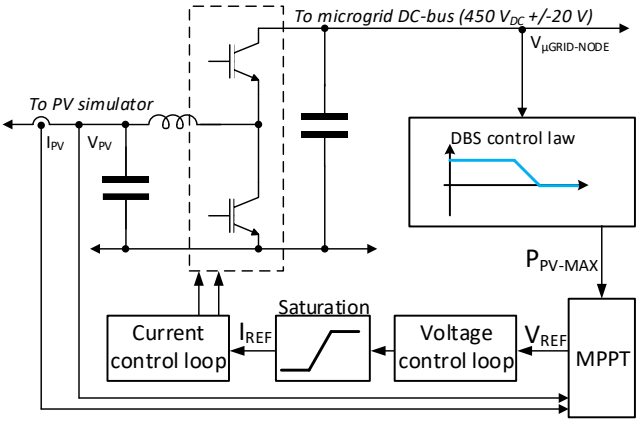

Fig 10: Solar energy generator: hardware and control scheme.

An electronic load (Chroma 63205A-1200-200) and fixed-value resistors are connected in the nodes to emulate different load transients. A 2,7 Ω planar resistor emulates the line impedance. Figure 11 shows the experimental test setup. All the equipment is connected through the experimental microgrid of the Industrial Electronic Systems Group (GSEI) of the Polytechnic University of Valencia, Spain (UPV) [30]. A set of tests has been carried out showing the performance of the proposed DBS laws.

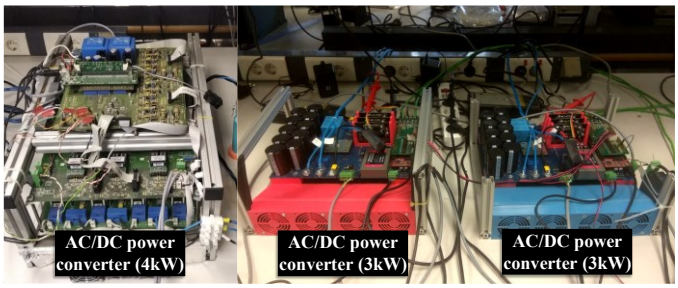

Fig 11: Experimental setup

B. Interlinking converters (DC power sources)

In the first test, the three DC power converters are programmed to behave as interlinking converters with the DBS control law of Figure 2.

Figure 12 depicts the stable behaviour of the output currents and voltage at the microgrid nodes of the power converters. In this figure, a 2,7 kW load is connected. Converter #3, connected to the same node as converter #2, delivers a slightly higher current because of its higher power rating. Converter #1, connected to node #1, is far from the load, so its current delivered is lower than those connected near the load (its node voltage is also higher). The power losses in the transmission line (2,7 Ω) are 4,6 W. If converters #1 and #2 were fully balanced and delivered the same current of #3, such power losses would be 10,8 W, doubling the inefficiency of the power transmission system.

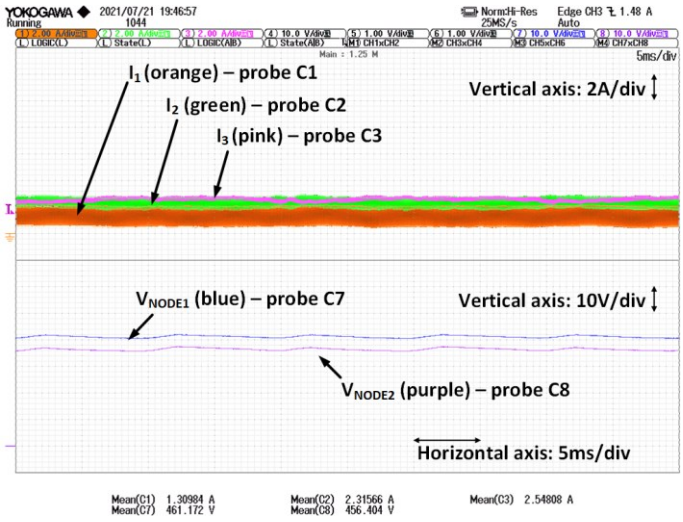

Fig 12: Microgrid's performance under 30% of the full power (73,3Ω@node2).

Figure 13 depicts the load profile used in the next test. An initial load of 2,7 kW@450 V_{DC} at node #2 drains the 30 % of the full microgrid power. Then, a load of 4 kW at node #1 causes a severe power-up step. After a while, the load at node #1 is disconnected, causing a power-down step.

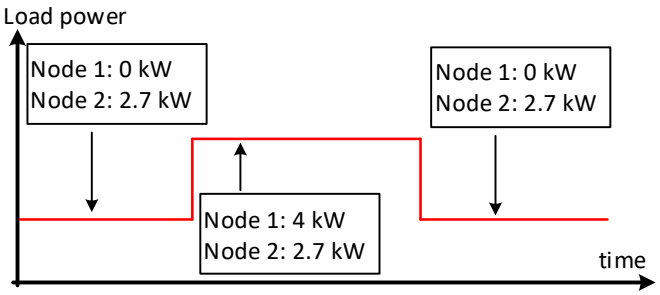

Fig 13: Load profile for testing DBS DC power sources.

A detailed view of the power transitions (figures 14 and 15) shows how stable and fast behaves the DBS technique (the voltage transition lasts only 40 ms in both experiments). Note that the current waveforms depicted are the output of the DC power converters, not the inductor current. Hence, the current ripple is due to the output capacitor.

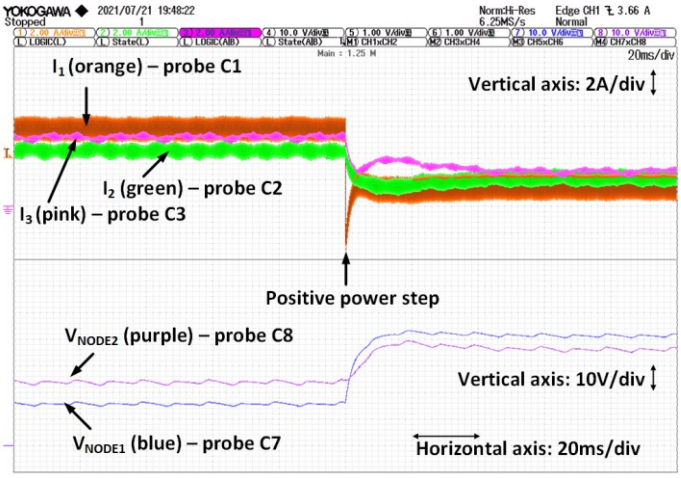

Fig 14: Positive power step (30% to 70% of the full power).

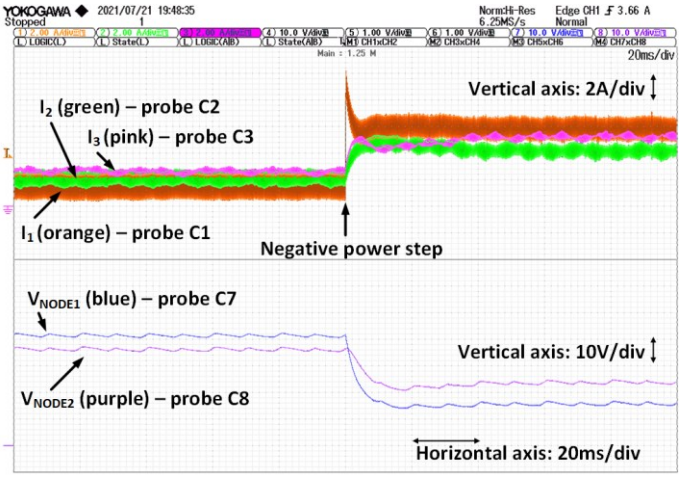

Fig 15: Negative power step (70% to 30% of the full power).

C. Plug-in Electrical vehicle (PEV) and other energy storage systems (ESS)

In the second test, the DC power converters #1 and #2 behave as interlinking converters (3 kW each) with the DBS control law from Figure 2. Converter #3 (4 kW) behaves as an ESS of a PEV, with the DBS control law of Figure 4. Figure

13 shows the load profile used, the same as the previous test.

Figure 16 shows the performance exhibited by the converters. The microgrid loaded to 30% of its total capacity leads to a 441,6 V_{DC} voltage at node #2. Therefore, according to the DBS law depicted in Figure 4, the ESS (converter #3, pink trace) is idle and does not deliver any power. When the load demand increases, the ESS delivers power to support the microgrid. During the power-up step transient (figure 16), the ESS reaches a steady state operation in less than 60 ms.

At the end of the power-down step transient (figure 17) the ESS returns to an idle state. Both positive and negative voltage and current transients are smooth and stable.

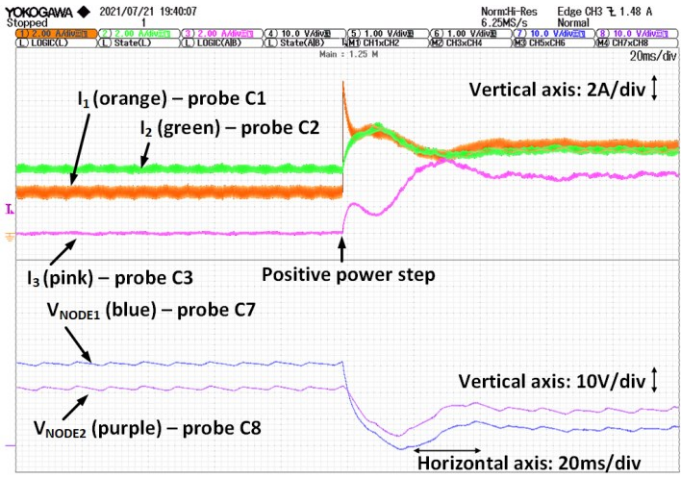

Fig 16: Positive power step (30% to 70% of the full power).

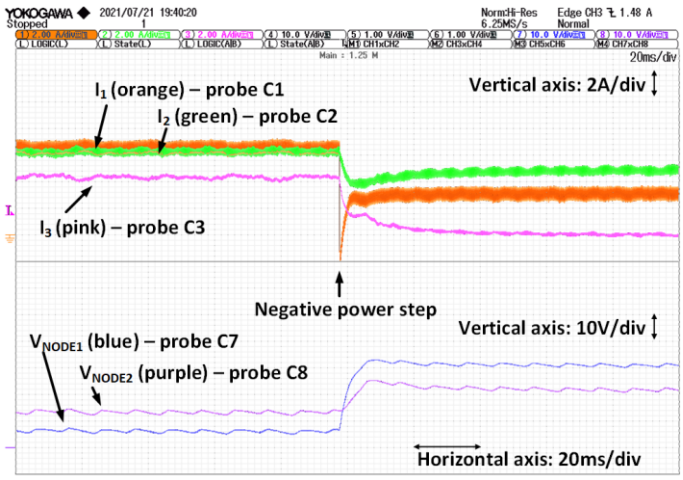

Fig 17: Negative power step (70% to 30% of the full power).

D. Plug-in Electrical vehicle (PEV) and other energy storage systems (ESS) discharge behaviour

Since the batteries are not infinite energy reservoirs, the ESS must deliver less power as time passes and the battery discharges. The ESS are only a transient power support for the microgrid, not a permanent one. In this test, the configuration of the converters is the same as in the previous one, but the ESS converter (converter #3) emulates a full discharge from 100% to 0% in 30 seconds (Figure 18).

This test begins with a 3,7 kW load in node #2, and the ESS does not contribute to supporting the microgrid. Then, the 4 kW resistive load is connected to node 1, and the ESS begins to deliver power to the microgrid. The power provided by the ESS decreases with the SoC of its battery. Once the ESS is empty, converters #1 and #2 must assume the full-load power. The dynamic variation of the maximum power of the ESS shows stable behaviour. Integrating this control technique with DBS DC power sources results in a smooth operation.

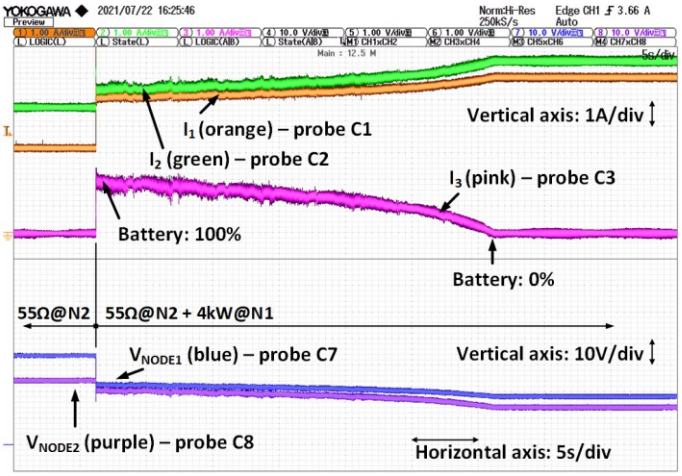

Fig 18: Battery discharge emulation.

E. Photovoltaic energy power converters

A PV generator running the MPPT algorithm under the proposed BDS law feeds the microgrid in this test. Also, a DBS-controlled ESS converter is connected to the microgrid.

First, the PV generator is OFF, and the ESS delivers the full load, green trace (figure 19). The PV generator turns on at a specific time, and the MPPT algorithm searches for the maximum power point (MPP). Hence, the output current of the PV converter (pink trace) increases up to the maximum value. In this test, the MPPT algorithm runs with a PV voltage step of 2.5 V and a running frequency of 10 Hz.

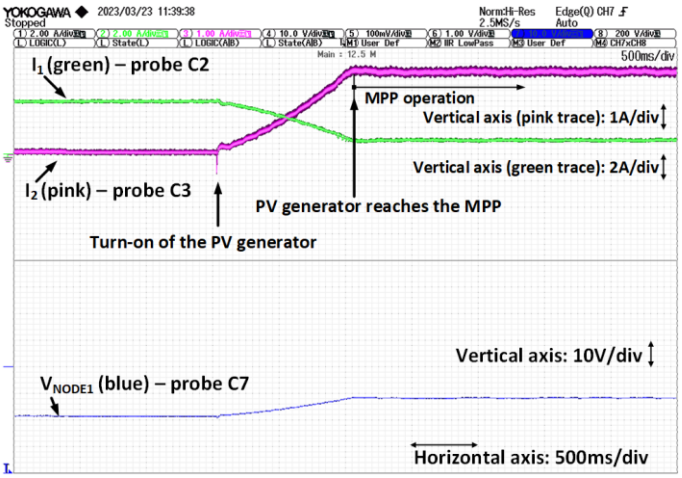

Fig 19: PV converter operation: reduction in the power provided by the ESS.

An additional test is performed (figure 20), in which the initial load of the microgrid is lower than in the previous case. As before, the PV converter reaches the MPP and the ESS,

initially delivering power to the microgrid, switches to the charging battery mode and drains the excess power between the PV converter and the load consumption.

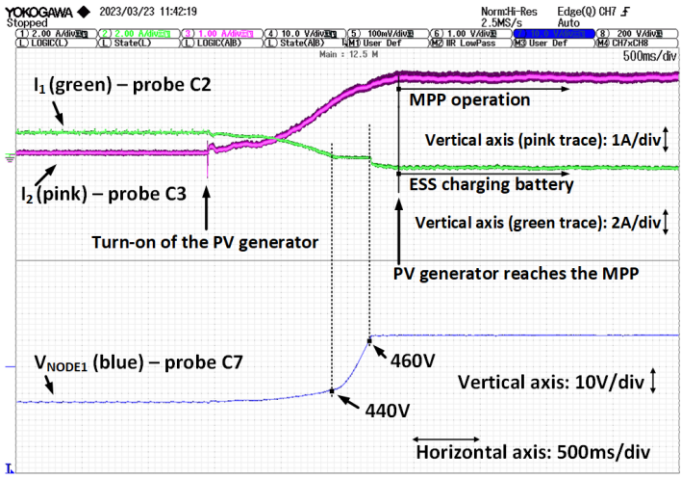

Fig 20: PV converter operation: ESS changes from delivering power to charging battery mode.

Figure 21 shows the behaviour of the power limitation of the PV generator. In this test, the load in the microgrid is reduced at a specific time. Hence, the voltage in the microgrid increases (blue trace). Following the DBS control law, the PV generator limits its output power (pink trace), and the ESS increases the charging current to its maximum value (green trace, negative values mean charging current). When the load of the microgrid rises again, the PV converter MPPT algorithm searches for the MPP again without limitations (figure 22).

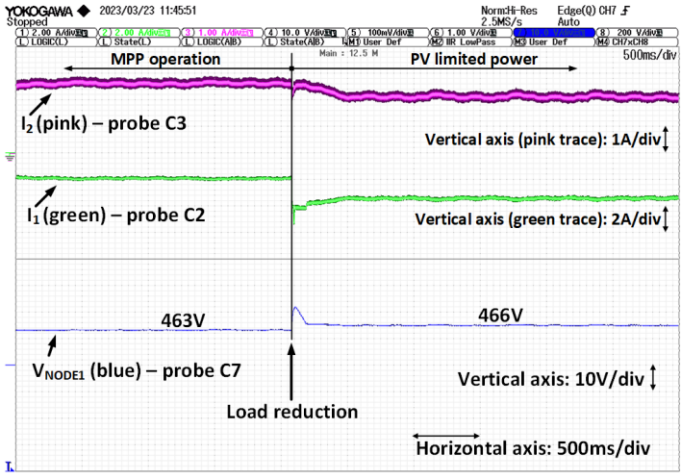

Fig 21: Load reduction in the microgrid: the PV converter limits its output power, and the ESS charges at full power.

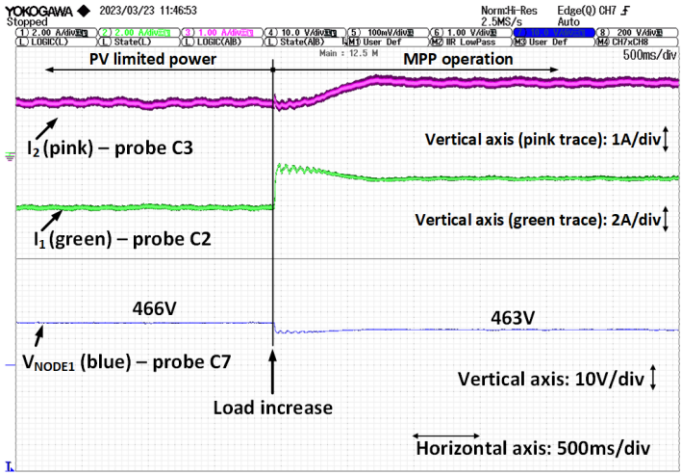

Fig 22: Increase in the microgrid load, the PV converter can now track the MPP without power constraints.

Additionally, we have tested an irradiance ramp variation. An initial irradiance level of 200 W/m^2 rises to 800 W/m^2 at a constant rate in 10 s, then the irradiance level remains constant for another 10 s; finally, it returns to 200 W/m^2 with the same slope. Figure 23 shows the experimental results. As the irradiance increases, the current of the PV generator (pink trace) rises, following the MPP consign. As PV power increases, the power delivered by the interlinking converter (orange trace) is reduced. Thus, following the DBS law, the voltage increases. Consequently, the current delivered by the DC generator decreases. When the irradiance decreases, the PV generator searches for the new MPP, delivering less power and, therefore, the microgrid's voltage decreases. Thus, the interlinking converter delivers more power, following the DBS law.

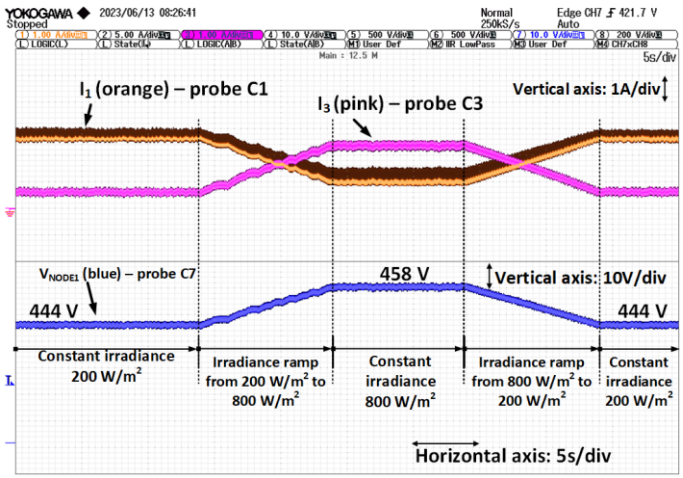

Fig 23: Irradiance ramp test.

F. Load priority levels

Figure 24 shows the load priority levels test results using a pair of DBS DC power sources (converters #1 and #2) and an ESS (converter #3). The ESS converter emulates a full battery discharge in 30 s. As in the previous test, the initial load is 3,7 kW@450 V_{DC} in node #2 (priority level 0), and the ESS is idle. A 2,4 kW load (priority level 1, must be disconnected at

voltages lower than 435 V_{DC}) connects in node #1 at a specific time, and now the ESS delivers power to the microgrid.

As the battery discharges, the ESS reduces its output power. Hence, the power delivered by converters #1 and #2 increases as the voltage decreases. When the voltage at node #1 falls below 435 V_{DC}, the 2,4 kW level 1 load self-disconnects and avoids the collapse of the microgrid.

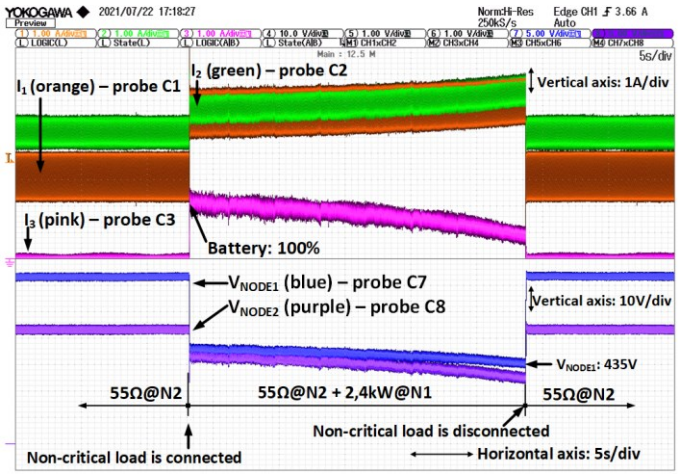

Fig 24: Load priority levels emulation.

It is worth pointing out that a specific procedure for the microgrid start-up is not needed, due to the following reasons: i) loads are automatically disconnected when the voltage is insufficient, and ii) converters running the DBS law behave as current sources during the start-up of the microgrid. Despite this, the DC-link capacitors of the converters should be precharged to avoid overcurrents. However, this issue does not concern the operation of the microgrid or DBS, but the converter itself.

To exemplify this, we've carried out a start-up test in which an interlinking converter will supply an initially unpowered microgrid with a critical load (level 0) demanding to be connected.

Initially, the interlinking converter is not running but the DC-link capacitors are precharged through the diodes. In such conditions, the load can not be feeded as the microgrid is unpowered and there is insufficient voltage. The DBS-controlled interlinking converter is turned on at a specific time, feeding the microgrid, so that the microgrid DC voltage can rise. As soon as the voltage reaches 430 V_{DC}, the critical load auto connects, and the interlinking converter feeds the required power. Figure 25 shows the test waveforms for the bus voltage (blue trace) and the current provided by the interlinking converter (orange trace).

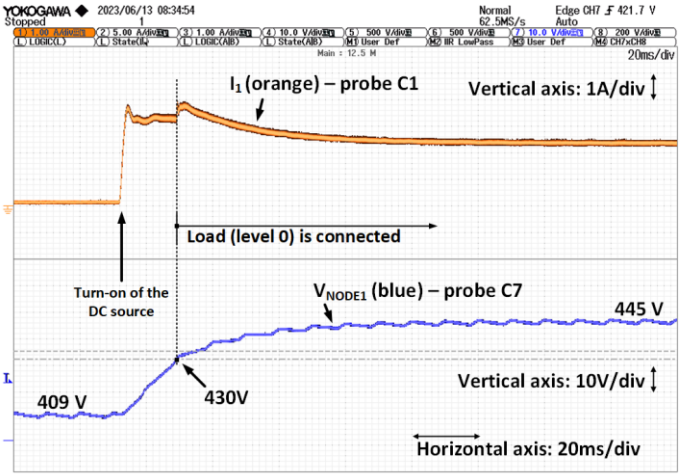

Fig 25: Example of Microgrid start-up.

V. CONCLUSION

This paper presents a control technique for the management of the agents connected to DC microgrids, which is based on DBS. The proposed control law for the different agents in a microgrid (interlinking converters, photovoltaic generators, ESS and loads) fits the agents' requirements and improve the microgrid's robustness.

The integration of renewable energy sources in a microgrid is a major challenge. The operation of a microgrid must guarantee that renewable sources operate at their full available power, using other non-renewable sources only when sufficient power is not available to supply the loads. When the renewable energy sources provide excess power, the microgrid should charge the ESS. This paper demonstrates the behaviour of a modified P&O algorithm and a DBS law for integrating PV generators in the microgrid. The resulting behaviour is satisfactory in harvesting the maximum available power and limiting its production as it is required.

Thus, the use of ESS is a crucial issue in microgrids. These systems improve the harvesting of renewable energy sources, enhance the exploitation cost of the microgrid (stores energy almost for free) and provide stability support.

Moreover, in a low-voltage microgrid, the grid impedance is mainly resistive. Hence, the power-sharing depends on the distance between each converter and the load: the power converters near the load deliver more power than those farther, thus reducing the power losses in the transmission lines.

Tests have been carried out on an experimental microgrid showing satisfactory results, with a smooth transient response for the microgrid DC voltage and good stability. Several combinations of agents have been tested in an experimental DC microgrid performing realistic scenarios. Even the start-up of the microgrid has been tested and demonstrated to be a stable and safe transient.

The proposed DBS technique has proven to be a suitable alternative to coordinate several agents in a microgrid in a robust and stable way, without the need for communication links.

REFERENCES

[1] D. A. Perez-DeLaMora, J. E. Quiroz-Ibarra, G. Fernandez-Anaya, and E. G. Hernandez-Martinez, "Roadmap on community-based microgrids deployment: An extensive review," Energy Reports, vol. 7, pp. 2883–2898, 2021, doi: https://doi.org/10.1016/j.egyr.2021.05.013.

[2] B. Moran, "Microgrid load management and control strategies," in 2016 IEEE/PES Transmission and Distribution Conference and Exposition (T&D), 2016, pp. 1–4, doi: 10.1109/TDC.2016.7520025.

[3] A. B. Shyam, S. R. Sahoo and S. Anand, "Voltage Regulation and Load Sharing in DC Microgrid Using Single Variable Global Average Estimation," in IEEE Journal of Emerging and Selected Topics in Industrial Electronics, doi: 10.1109/JESTIE.2023.3317800.

[4] Y. Rajbhandari et al., "Load prioritization technique to guarantee the continuous electric supply for essential loads in rural microgrids," Int. J. Electr. Power Energy Syst., vol. 134, p. 107398, 2022, doi: https://doi.org/10.1016/j.ijepes.2021.107398.

[5] C. Albea, C. Bordons, and M. A. Ridao, "Robust hybrid control for demand side management in islanded microgrids," IEEE Trans. Smart Grid, p. 1, 2021, doi: 10.1109/TSG.2021.3101875.

[6] A. Bani-Ahmed, M. Rashidi, A. Nasiri, and H. Hosseini, "Reliability Analysis of a Decentralized Microgrid Control Architecture," IEEE Trans. Smart Grid, vol. 10, no. 4, pp. 3910–3918, 2019, doi: 10.1109/TSG.2018.2843527.

[7] D. Wang, J. Yang, and S. Lin, "Analysis on transmission characteristics of broadband power line carrier and power frequency integrated communication for new energy microgrid," in 2017 7th IEEE International Conference on Electronics Information and Emergency Communication (ICEIEC), 2017, pp. 300–303, doi: 10.1109/ICEIEC.2017.8076567.

[8] M. Cintuglu and D. Ishchenko, "Multiagent-Based Dynamic Voltage Support of Power Converters During Fault Ride-Through," in IEEE Journal of Emerging and Selected Topics in Industrial Electronics, vol. 3, no. 3, pp. 549-558, July 2022, doi: 10.1109/JESTIE.2021.3119998.

[9] G. H. F. Fuzato et al., "Droop K-Sharing Function for Energy Management of DC Microgrids," in IEEE Journal of Emerging and Selected Topics in Industrial Electronics, vol. 2, no. 3, pp. 257-266, July 2021, doi: 10.1109/JESTIE.2021.3074889.

[10] H. Beder, B. Mohandes, M. S. E. Moursi, E. A. Badran, and M. M. E. Saadawi, "A New Communication-Free Dual Setting Protection Coordination of Microgrid," IEEE Trans. Power Deliv., vol. 36, no. 4, pp. 2446–2458, 2021, doi: 10.1109/TPWRD.2020.3041753.

[11] J. M. Guerrero, J. C. Vasquez, J. Matas, L. G. De Vicuña, and M. Castilla, "Hierarchical control of droop-controlled AC and DC microgrids - A general approach toward standardization," IEEE Trans. Ind. Electron., vol. 58, no. 1, pp. 158–172, Jan. 2011, doi: 10.1109/TIE.2010.2066534.

[12] S. Sharma, V. M. Iyer and S. Bhattacharya, "An Optimized Nonlinear Droop Control Method Using Load Profile for DC Microgrids," in IEEE Journal of Emerging and Selected Topics in Industrial Electronics, vol. 4, no. 1, pp. 3-13, Jan. 2023, doi: 10.1109/JESTIE.2022.3208513.

[13] J. Bryan, R. Duke, and S. Round, "Decentralized generator scheduling in a nanogrid using DC bus signaling," in IEEE Power Engineering Society General Meeting, 2004., 2004, pp. 977-982 Vol.1, doi: 10.1109/PES.2004.1372983.

[14] J. Schonbergerschonberger, R. Duke, and S. D. Round, "DC-Bus Signaling: A Distributed Control Strategy for a Hybrid Renewable Nanogrid," IEEE Trans. Ind. Electron., vol. 53, no. 5, pp. 1453–1460, 2006, doi: 10.1109/TIE.2006.882012.

[15] F. Li, Z. Lin, Z. Qian, and J. Wu, "Active DC bus signaling control method for coordinating multiple energy storage devices in DC microgrid," in 2017 IEEE Second International Conference on DC Microgrids (ICDCM), 2017, pp. 221–226, doi: 10.1109/ICDCM.2017.8001048.

[16] F. Li, Z. Lin, H. Xu and R. Wang, "A Review of DC Bus Signalling Control Methods in DC Microgrids," 2022 IEEE International Power Electronics and Application Conference and Exposition (PEAC), Guangzhou, Guangdong, China, 2022, pp. 1286-1291, doi: 10.1109/PEAC56338.2022.9959577.

[17] J. Schonberger, S. Round and R. Duke, "Autonomous Load Shedding in a Nanogrid using DC Bus Signalling," IECON 2006 - 32nd Annual Conference on IEEE Industrial Electronics, Paris, France, 2006, pp. 5155-5160, doi: 10.1109/IECON.2006.347865.

[18] C. N. Papadimitriou, V. A. Kleftakis, A. Rigas and N. D. Hatziargyriou, "A DC-microgrid control strategy using DC- bus signaling," MedPower 2014, Athens, 2014, pp. 1-8, doi: 10.1049/cp.2014.1667.

[19] K. Sun, L. Zhang, Y. Xing and J. M. Guerrero, "A Distributed Control Strategy Based on DC Bus Signaling for Modular Photovoltaic Generation Systems With Battery Energy Storage," in IEEE Transactions on Power Electronics, vol. 26, no. 10, pp. 3032-3045, Oct. 2011, doi: 10.1109/TPEL.2011.2127488.

[20] F. Li, Z. Lin, Z. Qian, J. Wu and W. Jiang, "A Dual-Window DC Bus Interacting Method for DC Microgrids Hierarchical Control Scheme," in IEEE Transactions on Sustainable Energy, vol. 11, no. 2, pp. 652-661, April 2020, doi: 10.1109/TSTE.2019.2900617.

[21] J. M. Guerrero, M. Chandorkar, T. Lee, and P. C. Loh, "Advanced Control Architectures for Intelligent Microgrids—Part I: Decentralized and Hierarchical Control," IEEE Trans. Ind. Electron., vol. 60, no. 4, pp. 1254–1262, 2013, doi: 10.1109/TIE.2012.2194969.

[22] I. Patrao, M.Liberos, E.Torán, R. González-Medina, E,Figueres, G.Garcerá. "Coordination of different agents in a microgrid using DC-Bus Signaling" in 1st IEEE Industrial Electronics Society Annual On-Line Conference (ONCON) 2022. ISBN 979-8-3503-9806-9

[23] J. Miret, M. Castilla and À. Borrell, "Voltage Support using Electric Vehicles in an Islanded Resistive-Microgrid under Voltage Sags," 2022 IEEE 31st International Symposium on Industrial Electronics (ISIE), Anchorage, AK, USA, 2022, pp. 32-38, doi: 10.1109/ISIE51582.2022.9831715.

[24] P. S. Subudhi, S. Padmanaban, F. Blaabjerg and D. P. Kothari, "Design and Implementation of a PV-Fed Grid-Integrated Wireless Electric Vehicle Battery Charger Present in a Residential Environment," in IEEE Journal of Emerging and Selected Topics in Industrial Electronics, vol. 4, no. 1, pp. 78-86, Jan. 2023, doi: 10.1109/JESTIE.2022.3195087.

[25] Y. Shen, T. He, D. Liu, Y. Tang and Y. Wang, "e-CNY Vehicle-to-Grid Real-time Settlement System," in IEEE Journal of Emerging and Selected Topics in Industrial Electronics, doi: 10.1109/JESTIE.2023.3303833.

[26] C. Pang, P. Dutta, and M. Kezunovic, "BEVs/PHEVs as Dispersed Energy Storage for V2B Uses in the Smart Grid," IEEE Trans. Smart Grid, vol. 3, no. 1, pp. 473–482, 2012, doi: 10.1109/TSG.2011.2172228.

[27] Z. Wang and S. Wang, "Grid Power Peak Shaving and Valley Filling Using Vehicle-to-Grid Systems," IEEE Trans. Power Deliv., vol. 28, no. 3, pp. 1822–1829, 2013, doi: 10.1109/TPWRD.2013.2264497.

[28] D. Routray, P. K. Rout and B. K. Sahu, "A brief review and comparative analysis of two classical MPPT techniques," 2021 International Conference in Advances in Power, Signal, and Information Technology (APSIT), Bhubaneswar, India, 2021, pp. 1-6, doi: 10.1109/APSIT52773.2021.9641301.

[29] "Technical Guide for Application of the Low-Voltage Electrical Regulation in Spain (in Spanish)," 2003. https://industria.gob.es/Calidad-Industrial/seguridadindustrial/instalacionesindustriales/baja-tension/Paginas/guia-tecnica-aplicacion.aspx (accessed March. 25, 2023).

[30] R. Salas-Puente, S. Marzal, R. González-Medina, E. Figueres, and G. Garcerá, "An Algorithm for the Efficient Management of the Power Converters Connected to the DC Bus of a Hybrid Microgrid Operating in Grid-connection Mode," Electr. Power Components Syst., vol. 46, no. 9, pp. 1029–1043, May 2018, doi: 10.1080/15325008.2018.1469177.

Iván Patrao received the Ingeniero Industrial (M.Sc) and Dr.Ingeniería Electrónica (Ph.D) degrees from the Polytechnic University of Valencia (UPV) in 2009 and 2015, respectively.

In 2008 he was with the R&D department of Siliken, involved in the design of electronic systems applied to photovoltaic applications. Since 2009 he has been with the Industrial Electronics Systems Group (GSEI) of the Electronics Engineering Department of the UPV, where he is an Assistant Professor. His main research fields are power converter modelling and control, converters for renewable energy, transformerless inverters and integration of distributed energy sources in microgrids.

Enric Torán received the Ingeniero Industrial (M.Sc) and the Electronic Systems Engineering (M.Sc) degrees from the Universitat Politècnica de València (UPV) in 2019 and 2020, respectively.
From 2021 he is with the Industrial Electronics Systems Group (GSEI) from the Electronics Engineering Department, UPV, where he researches in power converters, microgrids, and converters for renewable energy sources. He is developing his PhD, which focuses on converters connected to very weak grids and improving the grid quality.

Raúl González-Medina was born in Valencia, Spain, in 1978. He received the Ingeniero Industrial (M.Sc.) degree and the Dr. en Ingeniería Electrónica (Ph.D.) degree from the Universidad Politécnica de Valencia (UPV) in 2005 and 2015, respectively.

In 2005, he joined the Department of Electronics Engineering, UPV, where he is currently an Associate Professor of power electronics. He is also involved with the Industrial Electronic System Group. His main research fields are power converters, modulation techniques, grid-connected inverters, and converters for renewable energy sources.

Marian Liberos was born in Valencia, Spain, in 1992. She received the Master's Degree in Electronic Systems Engineering (M.Sc) and the Ph.D degree in the Doctoral Programme in Electronic Engineering from the Universitat Politècnica de València, València, Spain, in 2016 and 2021, respectively.
She is an Assistant Professor in the UPV, Alcoi, 03801, Spain. Since 2015 she belongs to the Industrial Electronic System Group, where she researches in power converters, circulating currents in converters connected in parallel and active filters.

Emilio Figueres (S'98-A'00-SM'10) is with the Department of Electronic Engineering at UPV, where he started his academic career in 1996.

Since 2011 he is Full Professor and was Head of the Department from 2008 to 2016. Since 2005, he has been responsible for the UPV Ph.D. Program in Electronics Engineering.

His research interests are in power processing of renewable energy sources, microgrids, grid connected converters, and power management in electric vehicles, working closely with industry on these topics through more than 30 company-funded research contracts. He holds 7 patents about power electronics, 5 of them licenced by industrial companies.
He is co-author of more than 100 papers published in JCR-indexed journals and international conferences on power electronics and renewable energy. He was co-recipient of the best paper award at the IEEE INDUSTRIAL ELECTRONICS TRANSACTIONS in 2012.

Gabriel Garcerá received the PhD—degree in Electrical Engineering from the Universitat Politecnica de Valencia (UPV) in 1998.

He is currently a Full Professor in Power electronics at the UPV. His main research fields are in Power Electronics and its applications to renewable energy, distributed generation microgrids and electric vehicles. He is co-author of more than 100 papers about those topics in international journals and conferences, having advised 16 Ph.D. Thesis.
From 2004 to 2019, he was an Associate Editor of the IEEE Transactions on Industrial Electronics.

He has been working in more than 50 research projects with companies and academia, many of them dealing with photovoltaic power converters.